Elastic $n-^6$He Scattering and ^{7}He Resonant States in the No-Core Shell Model

I. A. Mazur[a,b], **A. M. Shirokov**[b,c,d], **I. J. Shin**[e], **A. I. Mazur**[b], **Y. Kim**[e], **P. Maris**[d] **and J. P. Vary**[d]

[a] *Center for Extreme Nuclear Matters, Korea University, Seoul 02841, Republic of Korea*
[b] *Department of Physics, Pacific National University, Khabarovsk 680035, Russia*
[c] *Skobeltsyn Institute of Nuclear Physics, Lomonosov Moscow State University, Moscow 119991, Russia*
[d] *Department of Physics and Astronomy, Iowa State University, Ames, IA 50011-3160, USA*
[e] *Rare Isotope Science Project, Institute for Basic Science, Daejeon 305-811, Republic of Korea*

Abstract

We present results of calculations of $n-^6$He elastic scattering phase shifts and resonances in ^{7}He. The calculations utilize the SS-HORSE method combined with *ab initio* no-core shell model calculations of the ^{7}He and ^{6}He nuclei with Daejeon16 and the JISP16 NN interactions.

Keywords: *Nucleon-nucleus scattering; resonances; SS-HORSE method; no-core shell model*

1 Introduction

A modern trend of nuclear theory is a development of methods for describing nuclear states in the continuum, resonances in particular, as well as the boundaries of nuclear stability and nuclei beyond the drip lines. Obviously, *ab initio* ("first-principles") approaches in this field are of primary importance. The only input for *ab initio* theoretical studies is the nucleon-nucleon (NN) and, if needed, three-nucleon ($3N$) interactions.

Currently there are a number of reliable methods for *ab initio* description of nuclear bound states (see, e. g., the review [1]). Prominent methods include the Green function's Monte Carlo [2], the no-core shell model (NCSM) [3], the coupled cluster method [4], etc. The NCSM calculations are utilized in this paper. The NCSM is a modern version of the nuclear shell model which does not introduce an inert core and includes the degrees of freedom of all nucleons of a given nucleus. The multi-particle wave function is expanded in a series of basis many-body oscillator functions (Slater determinants) which include all many-body oscillator states with total excitation quanta less or equal to some given value defined in terms of $N_{\max}$. This makes it

Proceedings of the International Conference 'Nuclear Theory in the Supercomputing Era — 2018' (NTSE-2018), Daejeon, South Korea, October 29 – November 2, 2018, eds. A. M. Shirokov and A. I. Mazur. Pacific National University, Khabarovsk, Russia, 2019, p. 310.

http://www.ntse.khb.ru/files/uploads/2018/proceedings/MazurI.pdf.

possible to separate completely the center-of-mass motion. The number of basis states increases very rapidly with number of nucleons A and with $N_{\max}$. The achievement of a reasonable accuracy of the NCSM calculations is primarily limited by the memory of available modern leadership-class supercomputers. Currently, NCSM applications are obtained for nuclei with the number of nucleons of about 20. As A increases, due to computational limits restricting basis space sizes, there is a greater need for extrapolations to estimate converged results.

However, the NCSM cannot be directly applied to the description of resonant states. Energies of resonant states are positive with respect to some threshold so that one needs to consider decay modes. Special methods taking into account the continuum are therefore needed for the description of resonances.

There are well-developed methods for *ab initio* description of continuum spectrum states based on Faddeev and Faddeev–Yakubovsky equations that are successfully applied in nuclear physics for systems with $A \leq 5$ nucleons (see, e. g., the review [1] and Ref. [5]). A very important breakthrough in developing *ab initio* theory of nuclear reactions in systems with total number of nucleons $A > 4$ was achieved by combining the NCSM and the resonating group method to built the so-called NCSM with continuum (NCSMC) approach [6] which has been applied to description of several nuclear systems with up to 11 [7] and very recently up to 12 nucleons [8]. Nuclear resonances can be considered also in the no-core Gamow shell model (GSM) [9]. However, these methods bring forth additional challenges for a numerical realization and the respective calculations become very demanding.

Recently we proposed the SS-HORSE method [10–14], which generalizes the NCSM to the continuum spectrum states. The SS-HORSE allows one to calculate the single-channel S-matrix and resonances by a simple analysis of NCSM eigenenergy behavior as a function of parameters of the many-body oscillator basis. The SS-HORSE extension of the NCSM was successfully applied to the calculation of the neutron–α and proton–α scattering and resonant states in the ^{5}He and ^{5}Li nuclei in Refs. [10, 14]; a generalization of this approach to the case of the democratic decay provided a description of a resonance in the system of four neutrons (tetraneutron) [15].

A brief review of the SS-HORSE method is presented in Section 2. Results for a single-channel neutron scattering by the ^{6}He nucleus and resonances in the ^{7}He nucleus are presented in Section 3.

2 SS-HORSE method

Consider a channel of neutron scattering by a nucleus with A nucleons. The phase shift calculations within the SS-HORSE approach start from the calculation of the set of the NCSM eigenenergies E_i^{A+1} with some set of the NCSM basis parameters $N^i_{\max}$ and $\hbar\Omega^i$ for the whole $(A+1)$-particle system, as well as of the ground state energies E_i^A of the target nucleus with the same $\hbar\Omega^i$ and the excitation quanta $N^i_{\max}$ or $N^i_{\max} - 1$ depending of the parity of the states of interest of the $(A+1)$-particle system. The respective relative motion energy is the difference

$$E_i = E_i^{A+1} - E_i^A. \qquad (1)$$

The phase shifts $\delta_\ell(E_i)$ at the eigenenergies E_i in the partial wave with the orbital momentum ℓ in the case of neutral particle scattering are calculated as [10–12]

$$\tan \delta_\ell(E_i) = -\frac{S_{\mathbb{N}^i+2,\ell}(E_i)}{C_{\mathbb{N}^i+2,\ell}(E_i)}. \tag{2}$$

Here $S_{n,\ell}(E)$ and $C_{n,\ell}(E)$ are the regular and irregular oscillator solutions for the free motion, their analytical expressions can be found in Refs. [16–18]; the oscillator quanta of the relative motion

$$\mathbb{N}^i = N^i_{\max} + N^{A+1}_{\min} - N^A_{\min}, \tag{3}$$

where $N^i_{\max}$ is the excitation quanta in the $(A+1)$-particle system in the current calculation, $N^{A+1}_{\min}$ and $N^A_{\min}$ are the minimal total oscillator quanta consistent with the Pauli principle in the $(A+1)$- and A-particle systems, respectively. The energies E_i depend, of course, on the NCSM basis parameters, $N^i_{\max}$ and $\hbar\Omega^i$. Therefore by varying these parameters (note, $\hbar\Omega$ appears in the definition of the functions $S_{n,\ell}$ and $C_{n,\ell}$) we can calculate the phase shifts in some energy interval. Next we perform the phase shift parameterization which makes it possible to calculate the S-matrix and its poles including those associated with the resonant states in the $(A+1)$-body system.

The phase shifts can be parameterized using the effective range function,

$$K(E) = \left(\sqrt{2\mu E}/\hbar\right)^{2\ell+1} \cot \delta_\ell(E), \tag{4}$$

where μ is the reduced mass of scattered particles. The function (4) has good analytical properties and may be expanded in Taylor series of energy E (the so-called effective range expansion),

$$K(E) = -\frac{1}{a_\ell} + \frac{\mu r_\ell}{\hbar^2} E + cE^2 + \dots, \tag{5}$$

where a_ℓ is the scattering length and r_ℓ is the effective range. The expansion (5) works well at low energies, however in a larger energy interval, in particular, in the region of a resonance, it may be inadequate since the phase shift may may take the values of 0, $\pm\pi$, $\pm 2\pi$, ..., when the effective range function $K(E)$, according to Eq. (4), tends to infinity. Therefore we express the effective range function as a Padé approximant,

$$K(E) = \frac{-1 + w_1^{(n)} E + w_2^{(n)} E^2 + \dots}{a_\ell + w_1^{(d)} E + w_2^{(d)} E^2 + \dots}. \tag{6}$$

Clearly, at low energies the Padé approximant (6) unambiguously transforms into the effective range expansion (5).

With any set of parameters $w_1^{(n)}$, $w_2^{(n)}$, ..., a_ℓ, $w_1^{(d)}$, $w_2^{(d)}$, ... parametrizing the effective range function $K(E)$ we can easily calculate the phase shifts $\delta_\ell(E)$ in the energy interval of interest and calculate the energies E_i^{th} using Eq. (2) for any combination of the NCSM parameters $N^i_{\max}$ and $\hbar\Omega^i$. These energies E_i^{th} are compared with the set of energies E_i obtained in the NCSM calculations; the optimal values of $w_1^{(n)}$, $w_2^{(n)}$, ..., a_ℓ, $w_1^{(d)}$, $w_2^{(d)}$, ..., parametrizing the effective range function, are found by minimizing the sum of squares of deviation of the sets of E_i^{th} and E_i with weights enhancing the contribution of energies obtained with larger $N_{\max}$ values,

$$\Xi_w = \sqrt{\frac{1}{p}\sum_{i=1}^{p}\left(\left(E_i^{th} - E_i\right)^2 \left(\frac{N_{\max}^i}{N_M}\right)^2\right)}. \tag{7}$$

Here p is the number of energy values and N_M is the largest value of $N_{\max}^i$ used in the fit. With the optimal set of the fit parameters $w_1^{(n)}$, $w_2^{(n)}$, ..., a_ℓ, $w_1^{(d)}$, $w_2^{(d)}$, ... we can use Eq. (4) and (2) to obtain a parametrization of the $\hbar\Omega$ dependencies of the eigenenergies E_i in any basis space $\mathbb{N}^i$.

The S-matrix and the effective range function $K(E)$ are related by a simple analytic formula. Therefore, after obtaining an accurate parametrization of $K(E)$, one can search numerically for the S-matrix poles in the complex energy plain. Some tricks useful to design a stable and fast numerical algorithm for the pole searches at complex energies, are described in Ref. [14]. By locating the S-matrix poles, we obtain energies E_r and widths Γ of resonances in the many-body nuclear system.

3 n−^{6}He scattering

We start from the NCSM calculations of the ^{6}He ground state energies E_i^6 with the Daejeon16 [19] and JISP16 [20] NN interactions with $N_{\max}$ up to 16 and $\hbar\Omega$ ranging from 8 to 50 MeV. Next we calculate the lowest eigenenergies E_i^7 of the $3/2^-$, $1/2^-$, $5/2^-$ and $1/2^+$ states in the ^{7}He nucleus with $N_{\max}$ up to 17 with the same interactions and the same $\hbar\Omega$ values.

We first consider calculations performed with the Daejeon16 NN interaction. The set of the relative motion energies E_i is calculated using Eq. (1). As an example, we present in the left panel of Fig. 1 the set of relative motion energies E_i in the $3/2^-$

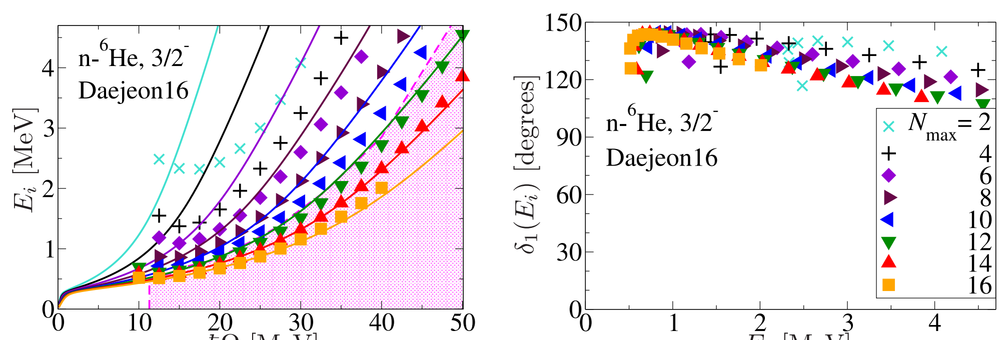

Figure 1: Left panel: Symbols are the energies of the relative motion E_i in the $3/2^-$ scattering state obtained in the NCSM with the Daejeon16 NN interaction; the energies used for the SS-HORSE parametrization are taken from the shaded area and the results of the SS-HORSE parametrization of energies for each $N_{\max}$ are shown by solid curves of respective colors. Right panel: The phase shifts calculated using Eq. (2) at the energies from the left panel.

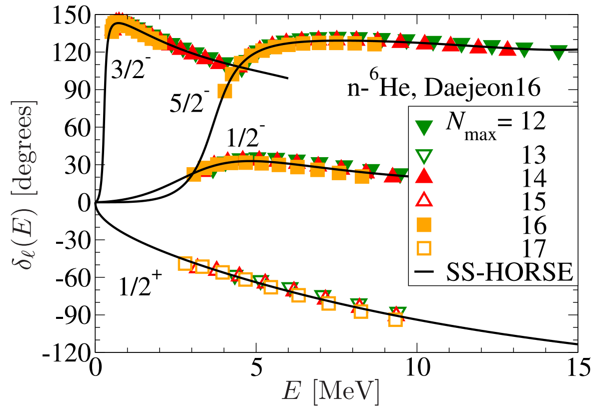

Figure 2: The phase shifts in the $3/2^-$, $1/2^-$, $5/2^-$ and $1/2^+$ scattering states obtained with the Daejeon16 NN interaction. Symbols are the selected phase shifts $\delta_\ell(E_i)$; the SS-HORSE fit of the phase shifts is presented by black curves.

state. The right panel of the same figure presents the set of the phase shifts $\delta_\ell(E_i)$ at these energies calculated using Eq. (2).

As stated in Refs. [10–15], we cannot use all energies E_i obtained by the NCSM for the further SS-HORSE analysis. The set of acceptable energies E_i should be selected for the SS-HORSE. In particular, the SS-HORSE equations are consistent only with those energies obtained at any given $N_{\max}$ which increase with $\hbar\Omega$, i. e., for any given $N_{\max}$ we should have $\frac{dE}{d\hbar\Omega} > 0$. In other words, from the set of energies $E_i^{N_{\max}}$ obtained by NCSM with any $N_{\max}$ we should select only those which are obtained with $\hbar\Omega > \hbar\Omega_{\min}^{N_{\max}}$, where $\hbar\Omega_{\min}^{N_{\max}}$ corresponds to the minimum of the $\hbar\Omega$ dependence of the relative motion energies $E_i^{N_{\max}}$.

Next, for the effective range function parametrization, we should select only the results obtained with large enough $N_{\max}$ and in the ranges of $\hbar\Omega$ values for each $N_{\max}$ where the phase shifts converge, at least, approximately. The phase shift convergence means that the phase shifts $\delta_\ell(E_i)$ obtained with different $N_{\max}$ and $\hbar\Omega$ values form a single smooth curve as a function of energy. In the right panel of Fig. 1, we see that the phase shifts $\delta_\ell(E_i)$ tend to form a smooth curve as $N_{\max}$ increases in a range of moderate energies which correspond to moderate $\hbar\Omega$ values. The phase shifts $\delta_\ell(E_i)$ obtained with small enough $N_{\max}$ deviate significantly from this single curve in large energy intervals. Correspondingly, the phase shifts obtained even with large $N_{\max}$ at small energies corresponding to small $\hbar\Omega$ values before the minima of the $\hbar\Omega$ dependences of $E_i^{N_{\max}}$ also deviate from the phase shift curve formed by the NCSM results from other $N_{\max}$ values.

The energies selected for the SS-HORSE fit are shown by the shaded area in the left panel of Fig. 1. The solid curves in this panel show the parametrization of the NCSM energies through the function (6) with a set of fitted parameters. The selected energies produce a set of the phase shifts $\delta_1(E_i)$ forming a smooth single curve, as is seen in Fig. 2, where we also present the SS-HORSE $3/2^-$ phase shifts accurately describing the set of the selected phase shifts $\delta_1(E_i)$.

We note that we perform a few alternative selections of energies E_i, e. g., we exclude from the selection some large energies E_i which lie far from the resonance. These alternative energy selections are used for estimating uncertainties of our predictions for the parameters of the resonance and low-energy scattering. The resonance energies E_r (relative to the $n + {}^6$He threshold) and widths Γ of resonances in the ^{7}He nucleus obtained by a numerical location of the S-matrix poles are presented in

Table 1: Energies E_r (relative to the $n + {}^6$He threshold) and widths of negative parity resonant states in ^{7}He nucleus and parameters of low-energy scattering $n-{}^6$He in positive and negative parity states, scattering lengths a_ℓ and effective ranges r_ℓ, obtained with Daejeon16 and JISP16 NN interactions. Our estimate of the uncertainties of the quoted results are in presented parentheses. The available results of the GSM calculations [21] and of the NCSMC calculations [22, 23] with SRG-evolved N^{3}LO chiral NN force together with experimental data are presented for comparison.

	Daejeon16	JISP16	GSM	NCSMC	Experiment		
$3/2^-$					[24]		
E_r, MeV	0.27(1)	0.70(2)	0.39	0.71	0.430(3)		
Γ, MeV	0.12(1)	0.60(2)	0.178	0.30	0.182(5)		
a_1, fm^3	−170(10)	−66(2)					
r_1, fm^{-1}	−1.10(3)	−0.88(1)					
$1/2^-$					[25]	[26]	[27]
E_r, MeV	2.7(1)	2.8(1)		2.39	3.03(10)	3.53	1.0(1)
Γ, MeV	4.2(1)	5.02(2)		2.89	2	10	0.75(8)
a_1, fm^3	−4.0(1)	−4.5(2)					
r_1, fm^{-1}	−4.4(2)	−3.1(1)					
$5/2^-$					[28]		
E_r, MeV	3.65(2)	4.37(4)	3.47(2)	3.13	3.35(10)		
Γ, MeV	1.37(1)	1.55(2)	2.25(28)	1.07	1.99(17)		
a_3, fm^7	−274(4)	−119(4)					
r_3, fm^{-5}	−0.0122(4)	−0.040(1)					
$1/2^+$							
a_0, fm	2.1(2)	3.2(5)					
r_0, fm	2.1(2)	1.1(6)					

Table 1 as well as the low-energy scattering parameters, the scattering length a_ℓ and the effective range r_ℓ, together with their estimated uncertainties. For comparison, we present in Table 1 also the resonance parameters from the GSM studies of Ref. [21] and the NCSMC studies of Refs. [22, 23] with SRG-evolved N^{3}LO chiral NN forces together with available experimental data. Our results for the $3/2^-$ resonance are seen to be consistent with the GSM results and experiment.

The same approach is used to examine the $1/2^-$ and $5/2^-$ resonances in the ^{7}He nucleus. The results for the phase shifts together with selected phase shifts $\delta_1(E_i)$ are also shown in Fig. 2 while the resonance and low-energy scattering parameters are presented in Table 1.

We note that the convergence of the $1/2^-$ phase shits, where we obtain a wide resonance, is slower than in the case of the $3/2^-$ state. As a result, our predictions for the $1/2^-$ resonance energy and width tend to have larger uncertainties. The predictions for the low-energy scattering parameters for the $1/2^-$ case appear to have uncertainties comparable to the resonance parameter uncertainties.

The experimental situation for the $1/2^-$ resonance is not clear. While the resonant energies of Refs. [25, 26] are comparable, the widths are very different. Our results are in fair agreement with the NCSMC results and the neutron pickup and proton-removal reaction experiments [25] and definitely do not support the interpretation of experimental data on one-neutron knockout from ^{8}He of Ref. [27] advocating a

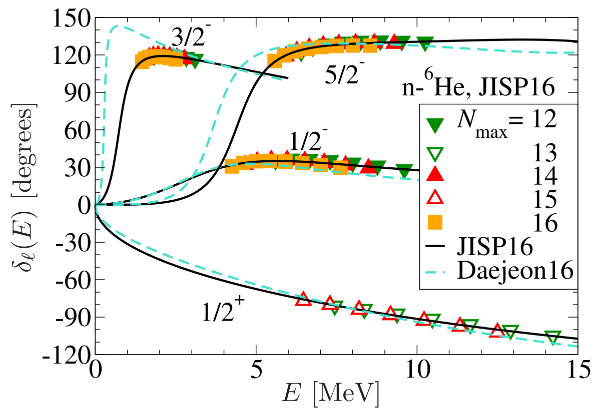

Figure 3: The phase shifts in the $3/2^-$, $1/2^-$, $5/2^-$ and $1/2^+$ scattering states obtained with the JISP16 NN interaction in comparison with those obtained with the Daejeon16 (red dashed curves). See Fig. 2 for other details.

low-lying ($E_r \sim 1$ MeV) narrow ($\Gamma \leq 1$ MeV) $1/2^-$ resonance in ^{7}He.

In the case of the $5/2^-$ scattering, the phase shifts convergence is similar to that of the $3/2^-$ state. The resonance energy and width presented in Table 1 are seen to be reasonably close to the experimental data, GSM and NCSMC results.

We analyze also the scattering in the $1/2^+$ state in our NCSM-SS-HORSE approach. The $1/2^+$ scattering phase shifts shown in Fig. 2 monotonically decrease without any signal of a resonant state. This result is in an agreement with the experimental data and the GSM predictions of Ref. [21] and NCSMC predictions [22, 23].

The phase shifts obtained with the JISP16 NN interaction are compared with those from Daejeon16 in Fig. 3. The only difference in getting these JISP16 results is that we avoided the expensive $N_{\max} = 17$ calculations for the positive-parity states since there is no experimental evidence for the positive-parity resonances in ^{7}He and we do not see any indication of such resonances in our phase shift calculations. The JISP16 and Daejeon16 $1/2^+$ scattering phase shifts are seen to be very close as are the respective low-energy scattering parameters listed in Table 1. The $3/2^-$ and $5/2^-$ ^{7}He resonances are generated by the JISP16 at slightly higher energies; the $1/2^-$ resonance appears approximately at the same energy, however its width is somewhat larger in the JISP16 results compared with the Daejeon16 results.

4 Summary and conclusions

We performed a study of the $n + {}^6$He continuum states within the single-channel SS-HORSE extension of the *ab initio* NCSM with JISP16 and Daejeon16 NN interactions. No resonance was found in the $1/2^+$ state consistent with the GSM [21], NCSMC [22, 23] studies and experimental situation. The $1/2^-$ resonance is predicted by both interactions to be wide enough and at the energy in a reasonable agreement with the NCSMC [22, 23] calculations and results of experiments of Refs. [25, 26] and clearly contradicts with the hypothesis of a low-lying narrow resonant state suggested in Ref. [27]. We note however that this as well as other ^{7}He resonances are known from the experiment with weak spin-parity assignment arguments. Our results for the narrow $3/2^-$ and wide $5/2^-$ resonances are in a reasonable agreement with experiment and with results quoted in the GSM [21] and NCSMC [22, 23] studies. However, JISP16 overestimates the width of the $3/2^-$ and the energy of the $5/2^-$ resonances.

Acknowledgements

This work is supported in part by the National Research Foundation of Korea (NRF) grant funded by the Korea government (MSIT) (No. 2018R1A5A1025563), by the Russian Science Foundation under Grant No. 16-12-10048, by the U.S. Department of Energy under Grants No. DESC00018223 (SciDAC/NUCLEI) and No. DE-FG02-87ER40371, by the Rare Isotope Science Project of the Institute for Basic Science funded by Ministry of Science and ICT and National Research Foundation of Korea (2013M7A1A1075764). Computational resources were provided by the National Energy Research Scientific Computing Center (NERSC), which is supported by the Office of Science of the U.S. Department of Energy under Contract No. DE-AC02-05CH11231, and by the National Supercomputing Center of Korea with supercomputing resources including technical support (KSC-2018-COL-0002).

References

[1] W. Leidemann and G. Orlandini, Prog. Part. Nucl. Phys. **68**, 158 (2013).

[2] S. C. Pieper and R. B. Wiringa, Ann. Rev. Nucl. Part. Sci. **51**, 53 (2001).

[3] B. R. Barrett, P. Navrátil and J. P. Vary, Prog. Part. Nucl. Phys. **69**, 131 (2013).

[4] H. Kümmela, K. H. Lührmann and J. Zabolitzky. Phys. Rep. **36**, 1 (1978).

[5] R. Lazauskas, Phys. Rev. C **97**, 044002 (2018).

[6] P. Navrátil, S. Quaglioni, G. Hupin, C. Romero-Redondo and A. Calci, Phys. Scr. **91**, 053002 (2016).

[7] A. Calci, P. Navrátil, R. Roth, J. Dohet-Eraly, S. Quaglioni and G. Hupin, Phys. Rev. Lett. **117**, 242501 (2016).

[8] P. Navrátil, *Nuclear structure and dynamics from chiral forces*, talk given at the Int. Conf. 'Nuclear Theory in the Supercomputing Era — 2018' (NTSE-2018), October 29 – November 2, 2018, Daejeon, South Korea, http://ntse.khb.ru/files/uploads/2018/presentations/Navratil.pdf.

[9] G. Papadimitriou, J. Rotureau, N. Michel, M. Płoszajczak and B. R. Barrett, Phys. Rev. C **88**, 044318 (2013).

[10] A. M. Shirokov, A. I. Mazur, I. A. Mazur and J. P. Vary, Phys. Rev. C **94**, 064320 (2016).

[11] I. A. Mazur, A. M. Shirokov, A. I. Mazur and J. P. Vary, Phys. Part. Nucl. **48**, 84 (2017).

[12] L. D. Blokhintsev, A. I. Mazur, I. A. Mazur, D. A. Savin and A. M. Shirokov, Yad. Fiz. **80**, 102 (2017) [Phys. Atom. Nucl. **80**, 226 (2017)].

[13] L. D. Blokhintsev, A. I. Mazur, I. A. Mazur, D. A. Savin and A. M. Shirokov, Yad. Fiz. **80**, 619 (2017) [Phys. Atom. Nucl. **80**, 1093 (2017)].

[14] A. M. Shirokov, A. I. Mazur, I. A. Mazur, E. A. Mazur, I. J. Shin, Y. Kim, L. D. Blokhintsev and J. P. Vary, Phys. Rev. C **98**, 044624 (2018).

[15] A. M. Shirokov, G. Papadimitriou, A. I. Mazur, I. A. Mazur, R. Roth and J. P. Vary, Phys. Rev. Lett. **117**, 182502 (2016).

[16] H. A. Yamani and L. J. Fishman, J. Math. Phys, **16**, 410 (1975).

[17] S. A. Zaytsev, Yu. F. Smirnov and A. M. Shirokov, Teor. Mat. Fiz. **117**, 227 (1998) [Theor. Math. Phys. **117**, 1291 (1998)].

[18] J. M. Bang, A. I. Mazur, A. M. Shirokov, Yu. F. Smirnov and S. A. Zaytsev, Ann. Phys. (NY) **280**, 299 (2000).

[19] A. M. Shirokov, I. J. Shin, Y. Kim, M. Sosonkina, P. Maris and J. P. Vary, Phys. Lett. B **761**, 87 (2016).

[20] A. M. Shirokov, J. P. Vary, A. I. Mazur and T. A. Weber, Phys. Lett. B **644**, 33 (2007).

[21] Y. Jaganathen, R. M. Id Betan, N. Michel, W. Nazarewicz and M. Płoszajczak, Phys. Rev. C **96**, 054316 (2017).

[22] S. Baroni, P. Navrátil and S. Quaglioni, Phys. Rev. Lett. **110**, 022505 (2013).

[23] S. Baroni, P. Navrátil and S. Quaglioni, Phys. Rev. C **87**, 034326 (2013).

[24] Z. X. Cao *et al.*, Phys. Lett. B **707**, 46 (2012).

[25] A. H. Wuosmaa *et al.*, Phys. Rev. C **72**, 061301 (2005).

[26] P. Boutachkov *et al.*, Phys. Rev. Lett. **95**, 132502 (2005).

[27] M. Meister *et al.*, Phys. Rev. Lett. **88**, 102501 (2002).

[28] D. R. Tilley *et al.*, Nucl. Phys. A **708**, 3 (2002).